

Received October 25, 2020; reviewed; accepted December 29, 2020

Effect of compound phosphate collector on flotation separation of jamesonite from marmatite and insights into adsorption mechanism

Wei Qin Huang¹, Guohua Gu¹, Xiong Chen^{2,3}, Yanhong Wang¹

¹ School of Minerals Processing and Bio-engineering, Central South University, Changsha 410083, Hunan, China

² Guangdong Institute of Resource Comprehensive Utilization, Guangzhou 510650, Guangdong, China

³ State Key Laboratory of Rare Metals Separation and Comprehensive Utilization, Guangzhou, 510650, Guangdong, China

Corresponding authors: guguohua@126.com (G. Gu), 155601016@csu.edu.cn (X. Chen)

Abstract: Separating jamesonite and marmatite is difficult due to their similar response to traditional collectors. To improve the selectivity of the collector and simplify the reagent system, compound phosphate (MP) as a collector for the separation of jamesonite from marmatite was studied in this study. The flotation tests revealed that, compared with the most used butyl xanthate (BX), MP had the advantages of lower dosage and stronger selectivity under weak acid pulp. Under the optimum flotation conditions, a concentrate with the grade of 31.54% Pb, 6.93% Zn and the recovery of 89.87% Pb, 12.31% Zn could be obtained from mixed binary minerals flotation (mass ratio of 1:1). Adsorption, zeta potential, FT-IR and XPS analysis demonstrated that MP performed strong chemisorption on jamesonite surface while underwent weak physisorption on marmatite, this difference was responsible for the excellent selectivity of MP toward jamesonite flotation and weak collecting capacity to marmatite.

Keywords: compound phosphate, jamesonite, marmatite, flotation separation, adsorption mechanism

1. Introduction

Jamesonite ($\text{Pb}_4\text{FeSb}_6\text{S}_{14}$) is an important source of strategic metals lead and antimony (Reyes Perez et al., 2019), which often coexists with other sulfide minerals, such as pyrrhotite (Fe_{1-x}S), marmatite ($(\text{Zn,Fe})\text{S}$), etc. (Radosavljevic et al., 2016). Froth flotation is the most effective way to separate complex sulfide ores, the difference in mineral surface hydrophobicity is the key to flotation separation (Wang, 2016). To modify the minerals surface properties, flotation reagents are added. Xanthates, as the commonly used collector to enhance surface hydrophobicity of jamesonite, suffer from the disadvantages of poor selectivity, so inhibitors are often used to inhibit marmatite in practice (Chen et al., 2011; Wei et al., 2013). Therefore, it is necessary to find effective collectors with a superior selectivity for the separation of jamesonite and marmatite. Some people have carried out relevant research on this subject: Ma (Ma., 2006) used aromatic thiophenol collector to float jamesonite and marmatite and found o-aminothiophenol and p-chlorophenylthiol exhibited stronger collecting ability for marmatite against jamesonite; Sun (Sun et al., 2010) introduced a novel collector 2-aminothiophenol to separate marmatite and jamesonite by the process of restraining lead and floating zinc; Wang (Wang, 2009) investigated the effect of a new collector DT08 on the flotation behaviour of jamesonite and marmatite without copper sulfate activation, and found that DT08 can realize the full flotation of two minerals under neutral conditions. It can be concluded that the agents mentioned in the above studies have a strong ability to collect marmatite rather than jamesonite. Usually, in the flotation process of polymetallic sulfide ore, lead sulfide ore and zinc sulfide ore are separated in sequence (Öztürk et al., 2018; Chen et al., 2019), which means that the above-mentioned collectors cannot be applied industrially. Hence, it is urgent to find a collector with good collecting ability and strong selectivity for jamesonite to be suitable for the industrial separation process of jamesonite and marmatite.

In this study, a compound phosphate collector named MP was used to selectively separate jamesonite from marmatite. MP is a compound phosphate collector composed of ammonium butyl dithiophosphate, aniline dithiophosphate and sodium carbonate in the ratio of 1:1:1. MP contains -SH, -P=S and -P-S₂ functional groups, with strong collecting ability. Also, it is reported that -P=S and -P-S can combine with Pb atom on the surface of galena to form strong chemical adsorption (Zhong et al., 2015). Therefore, MP may be used for the flotation separation of jamesonite from marmatite in theory.

The flotation performance of MP was evaluated through micro-flotation tests of single minerals and artificially mixed minerals. Moreover, zeta potential measurements, adsorption measurements, Fourier transform infrared spectrum (FT-IR) and X-ray photoelectron spectra (XPS) were conducted to reveal the adsorption mechanism of MP on jamesonite surface. The findings assist with new reagent selection and theoretical support for promoting the flotation separation of jamesonite from marmatite.

2. Experimental

2.1. Materials and reagents

Pure jamesonite and marmatite samples were both obtained from Guangxi Province, China. The purity of jamesonite and marmatite was over 98%, determined by chemical analysis and X-ray diffraction analysis (XRD, Advance D8, Bruker Ltd., Switzerland) (Fig. 1). After crushing, grinding and screening, the minerals with particle size of -75 to +38 μm were used for flotation tests. Minerals with particle size less than 38 μm were used for zeta potential, FTIR and XPS analysis.

MP as collector was synthesized in the laboratory, which was composed of ammonium butyl dithiophosphate, aniline dithiophosphate and sodium carbonate in the ratio of 1:1:1. Butyl xanthate (BX) and Methyl isobutyl carbinol (MIBC) purchased from Zhuzhou Flotation Reagents Factory, Hunan (China) were used as collector and frother, respectively. Analytical grade reagent sulfuric acid (H₂SO₄) and sodium hydroxide (NaOH) were used as pH regulators. Deionized water was used for all experiments.

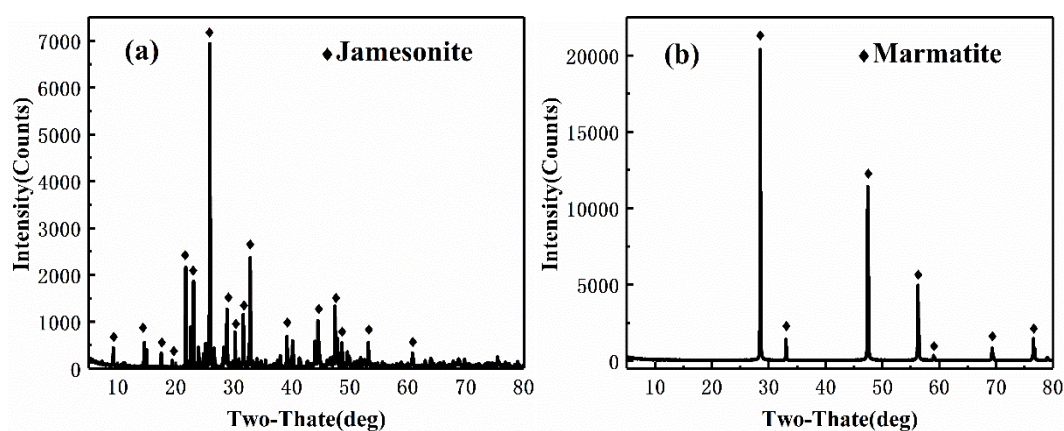


Fig. 1. XRD patterns of (a) jamesonite and (b) marmatite

2.2. Methods

2.2.1. Flotation tests

Flotation tests were performed in an XFG-type flotation machine at a spindle speed of 1860 rpm. For single mineral flotation tests, the sample (2.0 g) was cleaned by ultrasonication for 5 min, and then the supernatant was discarded after standing for 5 min. Finally, the sample was flushed into a flotation cell with 40 mL deionized water. The pulp pH was adjusted to the required value of 2, 4, 6, 8, 10, 12 by adding diluted H₂SO₄ or NaOH solution. Then the collector and frother were added sequentially for conditioning times of 3 and 1 min, respectively. Each flotation test was carried out for 3 min.

For artificially mixed minerals flotation tests, samples with 16.72 wt% Pb content consisted of pure jamesonite and marmatite with a mass ratio of 1:1. Recovery was calculated on the basis of product yields and Pb grades, which were assessed through chemical analysis.

2.2.2. Zeta potential measurements

Malvern Zeta sizer Nano ZS90 (England) was used to measure the zeta potential. The suspension consisting of 20 mg mineral sample with particle size less than 5 μm and 40 mL KCl electrolyte solution (0.001 mol L^{-1}) was agitated by magnetic stirrer for 3 min. Afterwards, the suspension was conditioned with or without MP at different pH values over the range of 2 to 12. The supernatant liquid was obtained for measurement after 10 min of settling. Each sample was conducted at least three times, and the averages were calculated as final results.

2.2.3. Adsorption measurements

The adsorption capacity was tested by TU-1810 UV-Vis spectrophotometer (Purkinje General, Beijing, China). 2 g of mineral sample and 40 mL of distilled water were transferred to a 100 mL Erlenmeyer flask. After adjusting the pH value of the slurry to the required test conditions, the collector MP was added, then stirred with a magnetic mixer for 30 min to ensure the adsorption process had reached equilibrium. After centrifugation of sample, the residual concentration of collector in the supernatant was determined by UV spectrophotometry and the adsorption capacity was calculated.

2.2.4. FT-IR spectroscopy analysis

FT-IR spectroscopy was conducted with KBr as the background by a Spectrum One (version BM) FT-IR (USA) spectrometer at 25°C. Purified minerals (1 g) were first ground to $-2 \mu\text{m}$, then conditioned with MP at pH 5.5 for 40 min. After being filtered, the solid samples were washed three times using distilled water, the samples were finally obtained by vacuum drying at 30 °C.

2.2.5. X-ray photoelectron spectroscopy (XPS) analysis

XPS analysis was carried out using k-alpha 1063 X-ray photoelectron spectrometer of Thermo Scientific (UK). The preparation step of natural and treated jamesonite was consistent with that in flotation tests tested at pH 5.5. The samples were filtered, washed three times by distilled water and vacuum dried at 30 °C. The final spectrums were calibrated by standard C 1s ($BE=284.80 \text{ eV}$).

3. Results and discussion

3.1. Flotation tests for single minerals

3.1.1. Effect of pH on single minerals flotation recovery

The effect of pH on jamesonite and marmatite flotation recovery with (a) BX (b) MP as collector are presented in Fig. 2 (a), (b), respectively. When using BX as collector, it can be seen from Fig. 2 (a) that the recovery of both jamesonite and marmatite experienced a decrease with the increase of pH value. It is worth mentioning that the recovery of jamesonite was higher than that of marmatite over the given pH range, indicating that the floatability of jamesonite was better than that of marmatite. However, the floatability difference was small at each pH value, the biggest deviation under pH 8.0, reaching 50%.

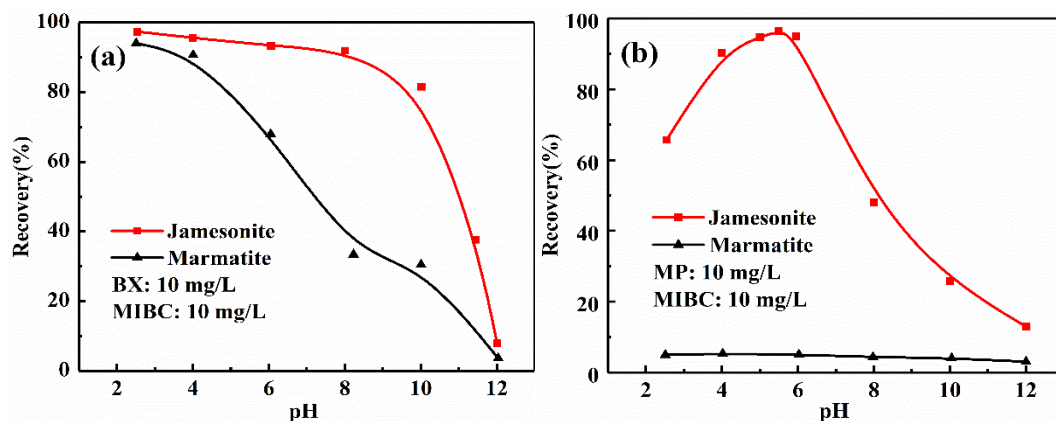


Fig. 2. Effect of pH on jamesonite and marmatite flotation recovery with (a) BX (b) MP as collector

demonstrating that BX collector was not efficiently enough to selectively separate jamesonite from marmatite. In this regard, we introduced a collector MP as an alternative to replace BX, and from Fig. 2 (b) it can be found that MP exhibited an excellent collecting ability and selectivity toward jamesonite rather than marmatite. The recovery of jamesonite increased gradually and then reached a plateau at pH around 5.5, reaching 95.46%. It can be noticed that the optimal pH range was between 4 and 6, a further increase of pH above 6 would lead to a lower recovery. Compared to jamesonite, however, marmatite maintained a rather low recovery around 7% throughout the pH range tested, which meant that selectively separation of jamesonite and marmatite could be achieved using MP as collector.

3.1.2. Effect of collector dosage on single minerals flotation recovery

Fig. 3 shows the effect of collector dosage on the flotation of jamesonite and marmatite. The results of Fig. 3 (a) meant that it was difficult to improve the flotation separation efficiency by adjusting BX dosage. On the contrary, as shown in Fig. 3 (b), the recovery of jamesonite was 85% higher than that of marmatite with increasing the dosage of MP until in excess of 10 mg/L, the recoveries of jamesonite decreased dramatically from 92.45% to 46.25%. The recovery of jamesonite reached the maximum value (95.18%) when the dosage of MP was 5 mg/L. The results indicated that low dosages of MP were beneficial to the flotation of jamesonite.

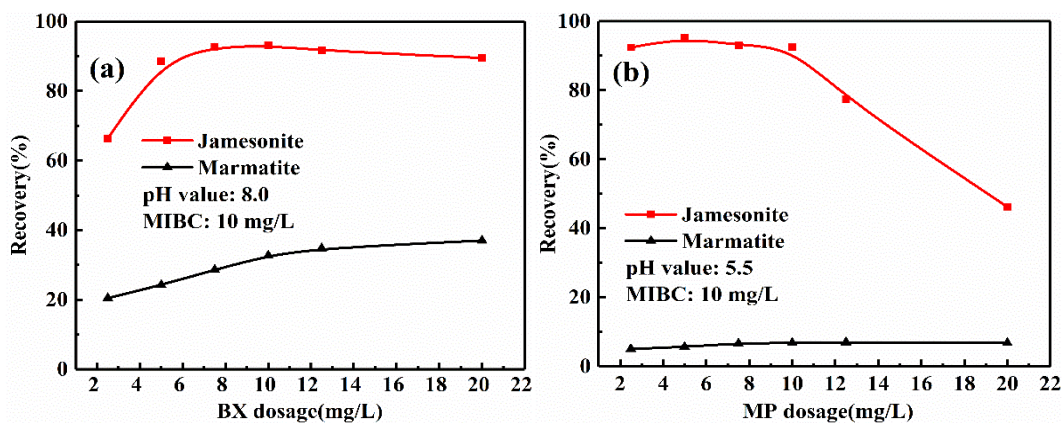


Fig. 3. Effect of (a) BX (b) MP dosage on jamesonite and marmatite flotation recovery

3.2. Flotation tests for artificial mixed minerals

Based on single mineral flotation test results, MP was issued as a promising selective collector used for the separation of jamesonite and marmatite. Therefore, the artificial mixed flotation tests were performed to further evaluate the selectivity of MP with MP dosage fixed at 5 mg/L and pH as variable.

As shown in Fig. 4, under the premise of 16.72% Pb content of mixed minerals, the concentrate grade of over 30% Pb with more than 89% recovery were obtained between pH 4.0 and 6.0. It is worth noting that the grade and recovery of Zn fluctuated around 6% and 11% respectively, illustrating MP selectively floated jamesonite in this pH range. Oppositely, ineffectively separation would be obtained when pH exceeded this range, reflecting MP should be used under conditions of low MP dosage and weak acid slurry.

3.3. Zeta potential analysis

Fig. 5 compares the zeta potential of jamesonite and marmatite in the presence or absence of MP at various pH values. As shown in Fig. 5, the bare jamesonite surface was negatively charged within the entire pH range tested and the isopotential point was not observed. In the presence of 5 mg/L MP, the zeta potential of jamesonite shifted towards a more negative direction compared with that of raw ore, which illustrated that electronegative MP was readily adsorbed onto the jamesonite surface. The remarkable difference occurred at pH 2.0~6.0, indicating adsorption was more prominent at this range which concurred with the flotation results. The zeta potential of untreated and MP-treated marmatite is shown in Fig. 5. The isoelectric point (IEP) of marmatite differed in various literatures due to the diffe-

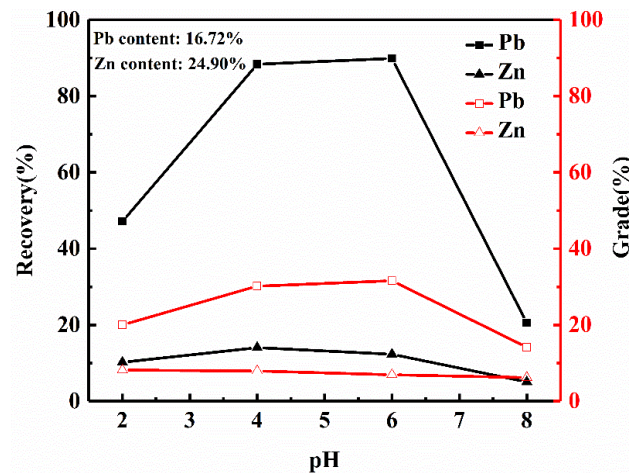


Fig. 4. Separation results of jamesonite from marmatite under different pH

rence in the extent of oxidation of sample surfaces and the amount of iron present in solid solution (Lai et al., 2019; Sui et al., 1998; Finkelstein, 1997; Zhang et al., 2014). Fig. 5 shows that the IEP of the pure marmatite without any flotation reagents in aqueous solutions is observed to be around pH 2.7. With the increase of pH value, the hydroxyl group adsorption on the metal sites was favoured, reducing the zeta potential of marmatite from 3.9 mV (pH 2.0) to -46.4 mV (pH 12.0) (Davila-Pulido et al., 2014). After MP treatment, the zeta potential only shifted slightly with increasing pH, indicating only a small amount of MP was adsorbed onto the marmatite surface over the whole pH range. This may be due to the competitive adsorption of MP and hydroxide ions. The increment in the negative zeta potential ($\Delta|\zeta|$) has been directly related to adsorption density of the ions at the solid/water interface (Zhang et al., 2014). It can be seen from Fig. 5 that the $\Delta|\zeta|$ of jamesonite was throughout larger than that of marmatite, which intuitively reflected that the adsorption density of MP on the jamesonite surface was greater than that on marmatite surface.

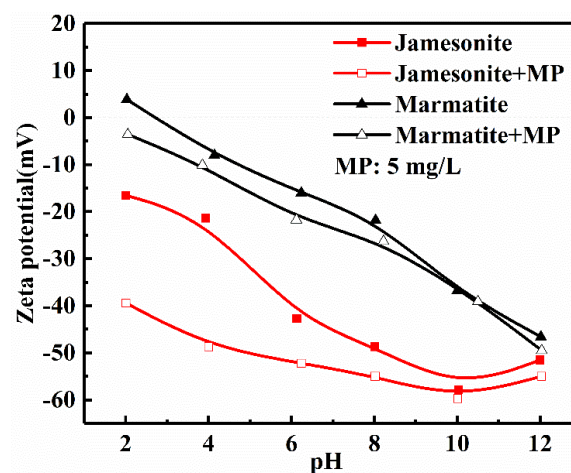


Fig. 5. Zeta potentials of jamesonite and marmatite in the presence or absence of MP as a function of pH

3.4. Adsorption measurements results

The adsorption capacity of the agent is often used in combination with the zeta potential to characterize the strength of the agent adsorption on the mineral surface. Fig. 6 shows the effect of pulp pH and MP dosage on the adsorption of jamesonite and marmatite. Obviously, the adsorption capacity of MP on jamesonite was much higher than that on marmatite, which was identical with the result of zeta potential. It can be seen from Fig. 6 (a) that the adsorption of MP on the surface of jamesonite was highest when the pH was 4.0~6.0, which indicates that MP prefers to adsorb in weak acid condition. As shown in Fig.6 (b), the adsorption capacity on jamesonite increased correspondingly with the enlargement of MP's dosage. The growth rate was fast until the dosage increased to 10 mg/L, which could be explained

by the weak alkalinity of MP. In other words, the pH value of the pulp rose when the dosage of MP increased to a certain extent, exceeding the optimal pH range of 5.5~6.0 for jamesonite flotation (Lager et al., 2015). Moreover, under the same conditions, regardless of the slurry pH value or MP dosage there was little effect on MP adsorption of marmatite. It may be that the huge difference in adsorption capacity of MP between jamesonite and marmatite results in its excellent selectivity. The difference in adsorption capacity is related to the properties of mineral surface, which will be further analysed by FT-IR and XPS.

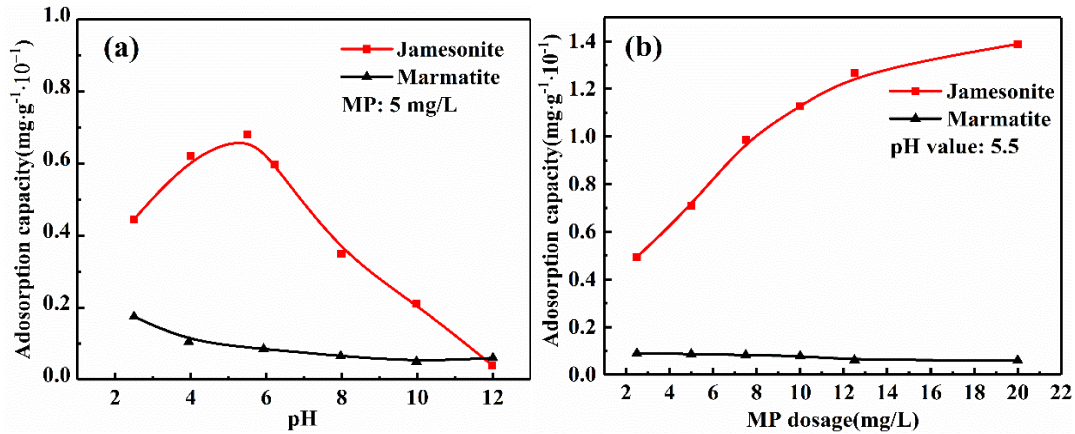


Fig. 6. Effect of (a) pH (b) MP dosage on the adsorption of jamesonite and marmatite

3.5. FT-IR spectra analysis

In Fig. 7 shows the FT-IR spectrum of MP. The characteristic adsorption peaks appearing at 2561.23 cm^{-1} and 2512.60 cm^{-1} were assigned to the stretching vibrations of $-\text{SH}$ (Huang et al., 2010), and stretching vibrations of $-\text{P}=\text{S}$ occurred on 1276.24 and 840.12 cm^{-1} (Ignatkina et al., 2013; Zhang et al., 2015). The peaks observed at 648.90 cm^{-1} and 542.78 cm^{-1} were attributed to the anti-symmetric stretching vibrations of $-\text{P}-\text{S}_2$ (Zhang et al., 2014). The peak at 3445.22 cm^{-1} was put down to asymmetrical stretching vibration of $-\text{NH}$ (Huang et al., 2010) and one peak located at 1493.56 cm^{-1} represented $-\text{CH}_3$ or $-\text{CH}_2-$ deformation vibration (Zhang et al., 2014).

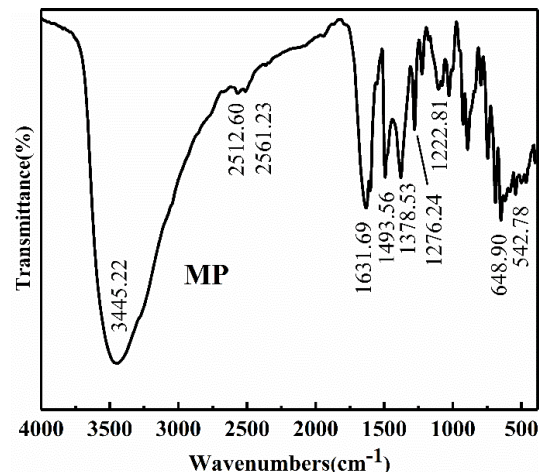


Fig. 7. FT-IR spectra of MP

To further understand the adsorption mechanism of MP, the FT-IR spectra of jamesonite and marmatite before and after MP treatment are shown in Fig. 8. It is reported that if the characteristic peaks of the reagent are not observed on the FT-IR spectrum of the mineral treated by the reagent, it means that the adsorption of the agent on the mineral surface is very likely to be physical adsorption (Zhao et al., 2019; Ming et al., 2020; Xiong et al., 2020). Conversely, if the characteristic peak of the reagent appears in the FT-IR spectrum after the interaction between the reagent and the mineral, or the wavenumber is shifted to a certain extent, it is considered that the chemisorption of the reagent on the

mineral surface has occurred (Zhao et al., 2021; Zhong et al., 2015; Cao et al., 2021). As shown in Fig. 8 (a), the characteristic peaks of bare jamesonite were observed at 977.35 cm^{-1} and 619.37 cm^{-1} (Sun et al., 2015; Zhang et al., 2015). After interaction with MP, these peaks migrated to 997.62 and 651.43 cm^{-1} , respectively. Moreover, from the MP-treated jamesonite spectrum, some new peaks associated with MP appeared at 1492.25 cm^{-1} (-CH₃ or -CH₂); 1146.72, 864.04 cm^{-1} (P=S); 587.59, 464.76 cm^{-1} (-P-S₂). It can be seen easily that the FT-IR spectrum of the jamesonite after conditioned with MP was basically consistent with the FT-IR spectrum of lead dibutyl dithiophosphate reported in the literature, demonstrating MP had strong chemisorption on jamesonite surface (Zhang et al., 2015). The main bands corresponding to the relevant chemical bond of MP was summarized in Table 1, which was of great importance for visually explaining the chemisorption between MP and jamesonite. As illustrated in Fig. 8 (b), the characteristic peaks of bare marmatite appeared at 634.74, 798.21 and 1105.33 cm^{-1} (Wei et al., 2019). After MP treatment, there were negligible changes on the spectra of marmatite, indicating MP was weakly adsorbed onto the marmatite surface. Therefore, we can reasonably speculate that physical adsorption process may dominate the interaction of MP with marmatite. According to the results of FT-IR spectra, it could be determined that MP had chemisorbed on jamesonite surface. However, for marmatite, it can only be preliminarily judged that MP might be physically adsorbed on the marmatite surface. Further analysis will be carried out through XPS, aiming to determine the atomic environment based on the core-level binding energy, to obtain the elemental composition and chemical state of the interaction product of the MP with the mineral surface.

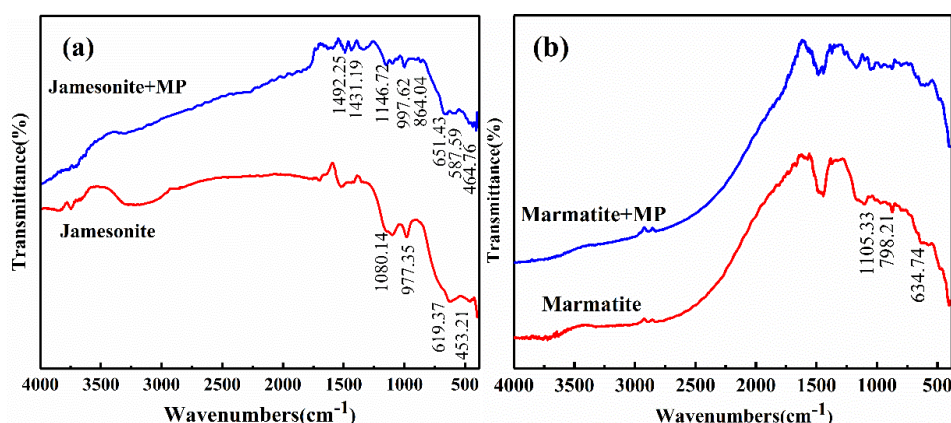


Fig. 8. FT-IR spectra of (a) jamesonite (b) marmatite before and after interacted with MP

Table 1. The bands corresponding to the relevant chemical bond of MP in FT-IR spectra

FT-IR	Band (cm^{-1})	Chemical Bond	Reference
MP	3445.22	N-H	(Huang et al., 2010)
	2561.23, 2512.60	S-H	(Ignatkina et al., 2013; Zhang et al., 2015)
	1493.56	-CH ₃ or -CH ₂ -	(Zhang et al., 2014)
	1276.24, 840.12	P=S	(Huang et al., 2010)
Jamesonite+MP	648.90, 542.78	P-S ₂	(Zhang et al., 2014)
	1492.25	-CH ₃ or -CH ₂ -	(Zhang et al., 2014)
	1146.72, 864.04	P=S	(Huang et al., 2010)
Jamesonite+MP	587.59, 464.76	P-S ₂	(Zhang et al., 2014)

3.6. XPS analysis

XPS is utilized to obtain more detailed information about the properties of minerals conditioned with MP. Table 2 gives the XPS numerical data of jamesonite with and without MP pre-processing. It can be seen that an element P with concentration 1.7% appears in the presence of MP, confirming the adsorption of MP on jamesonite surface.

Phosphates are prone to interacting with heavy metal ions to form insoluble salts, making minerals hydrophobic and easy to float (Zhang et al., 2015; Liu, 2009). To explore the interaction site of the surface

Table 2. Atomic concentration and binding energy of elements of jamesonite before and after MP treatment

Surface elements	Jamesonite		Jamesonite+MP	
	Atomic concentration/%	Binding Energy/eV	Atomic concentration /%	Binding Energy/eV
C1s	25.7	284.80	23.2	284.80
O1s	10.3	530.44	9.2	530.39
S2p	33.7	161.26	34.2	161.09
Sb3d5	17.1	529.36	16.6	529.32
Pb4f	9.9	137.81	11.9	138.42
Fe2p	3.3	710.21	3.2	710.19
P2p	-	-	1.7	132.29

of jamesonite treated by MP, the high-resolution XPS of Pb 4f and Sb 3d were analysed. The change in binding energy can judge whether metal elements participate in chemical reactions (Zhao et al., 2021).

As shown in Fig. 9 (A), the Pb 4f splits into Pb 4f_{7/2} and Pb 4f_{5/2} components. The peaks of Pb 4f_{7/2} spectrum of pure jamesonite at 137.81 eV and 138.78 eV correspond to Pb atom in Pb-S and Pb-O, respectively (Ma et al., 2016; Jia et al., 2019). After interacting with MP, the binding energy of these two peaks moved to 138.33 eV and 139.25 eV, respectively, indicating the electronic environment of the Pb atom had been changed which might result from the donation of electrons by Pb to MP (Jia et al., 2019). The result corroborated that MP reacted with Pb directly, which was in agreement with the result of FT-IR analysis.

As presented in Fig. 9 (B), Sb 3d overlapped with O1s which was located at around 530.44 eV (Cao et al., 2020). For pure jamesonite, the spectrum of Sb 3d_{5/2} was fitted into two peaks with binding energy of 529.36 eV and 530.56 eV, which were assigned to Sb-S and Sb-O, respectively (Zakaznova-Herzog et al., 2006). After adding MP, no new peak appeared and no significant shift occurred, indicating Sb sites on the jamesonite performed very weak responsiveness towards MP adsorption.

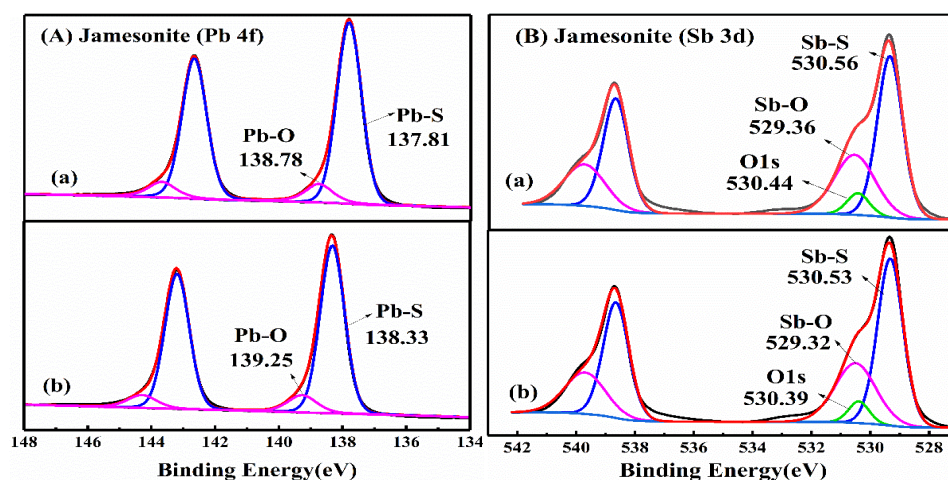


Fig. 9. High-resolution XPS of (A) Pb4f (B) Sb3d ((a)jamesonite before and (b) after MP treatment)

Table 3 displays the surface properties of marmatite before and after MP treatment. After interaction with MP, the relative atomic concentration of main elements C, Zn, O, S, on marmatite surface were almost unchanged. The high-resolution XPS of Zn 2p_{3/2}, S 2p of marmatite before and after MP treatment were in Fig. 10 (A), (B). The spectrum of Zn 2p_{3/2} on the surface of fresh marmatite could be divided into two peaks located at 1021.67 eV and 1022.58 eV, designated as Zn-S and Zn-O/OH, respectively (Feng et al., 2020; Ejtemaei et al., 2017). S 2p in pure marmatite was a typical doublet, and species at binding energy of 161.69 eV and 162.89 eV were assigned to S²⁻ of ZnS (Ejtemaei et al., 2017; Huang et al., 2019). After MP treatment, Zn 2p_{3/2} and S 2p shifted only by + 0.01 eV, which were within the instrumental error (0.2 eV), indicating that the adsorption between MP and marmatite was physical

instead of chemical (Pan et al., 2020; Liu et al., 2020; Cao et al., 2020). These results were in good agreement with the FT-IR results.

Based on FT-IR and XPS analysis, the results demonstrated that MP exhibited strong chemisorption on the jamesonite surface due to lead sites readily combine with MP, which had a positive effect on the jamesonite flotation. However, the negligible change in the binding energy of Zn indicated that Zn sites on the surface of marmatite were not sensitive to MP adsorption, which further corroborated MP was adsorbed on marmatite surface by weak physical adsorption.

Table 3. Atomic concentration and binding energy of elements of jamesonite before and after MP treatment

Surface elements	Marmatite		Marmatite +MP	
	Atomic concentration/%	Binding Energy /eV	Atomic concentration /%	Binding Energy /eV
C1s	27.9	284.80	26.7	284.80
O1s	12.2	531.67	12.3	531.65
S2p	28.7	161.71	29.5	161.72
Fe2p	7.0	709.78	7.1	709.75
Zn2p3	24.2	1021.67	24.4	1021.66

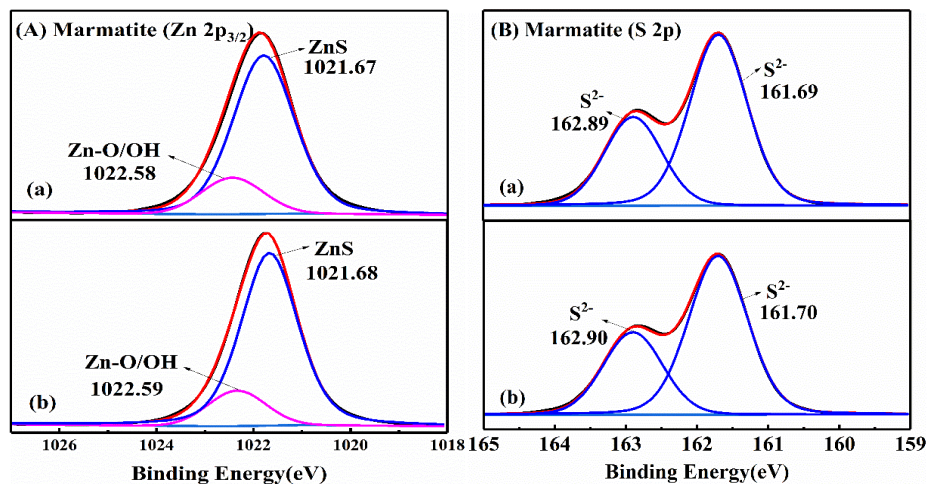


Fig. 10. High-resolution XPS of (A) Zn 2p_{3/2} (B) S 2p ((a)marmatite before and (b) after MP treatment)

4. Conclusions

Compound phosphate (MP) was employed as a collector in the flotation separation of jamesonite from marmatite without any depressant. Micro-flotation results showed that MP had the advantages of lower dosage and better selectivity than conventional collector BX. When MP dosage was 5 mg/L, the mixed minerals containing 16.72% Pb could be effectively separated with a Pb concentrate grading over 30% at a recovery of close to 90% under the weak acid pH range (4.0 to 6.0).

In addition, it is concluded from zeta potential, adsorption, FT-IR and XPS analysis that MP strongly adsorbed on jamesonite surface under weak acidity, while slightly adsorbed on marmatite surface in the whole pH. The interaction between MP and jamesonite was governed primarily by chemisorption, whereas that between MP and marmatite mainly occurred through weak physical adsorption. This is the reason why MP has excellent selectivity for jamesonite and poor collecting ability to marmatite. The research has important significance for the processing of lead-zinc ores.

Acknowledgments

The authors acknowledge the support of the National Key Technology R&D Program (No.2015BAB12B02); National Natural Science Foundation of China (No.52074358); GDAS' Project of Science and Technology Development (2020GDASYL-20200103104).

References

- REYES, PEREZ, M., PALACIOS, BEAS, E.G., BARRIENTOS, F.R., PEREZ, LABRA, M., JUAREZ, TAPIA, J.C., REYESDOMINGUEZ, I.A., FLORES GUERRERO, M.U., TEJA, RUIZ, M.A., GUTIERREZ, GARCIA, C.E., 2019. *Chemical and Instrumental Characterization of a Sulphosalt Lead Type Jamesonite*, *Minerals Metals & Materials Series*, 503-510.
- RADOSAVLJEVIC, S.A., STOJANOVIC, J.N., RADOSAVLJEVIC-MIHAILOVIC, A.S., VUKOVIC, N.S., 2016. *(Pb-Sb)-bearing sphalerite from the Cumavici polymetallic ore deposit, Podrinje Metallogenic District, East Bosnia and Herzegovina*, *Ore. Geol. Rev.*, 72(1), 253-268.
- WANG, G., 2016. *Mode-independent control of singular Markovian jump systems: A stochastic optimization viewpoint*, *Appl. Math. Comput.*, 286, 155-170.
- CHEN, J., LI, Y., LONG, Q., WEI, Z., CHEN, Y., 2011. *Improving the selective flotation of jamesonite using tannin extract*, *Int. J. Mineral Process.*, 100(1-2), 54-56.
- WEI, Z., WU, C., YU, Z., HUANG, R., MU, X., 2013. *Research The Several Organic Inhibitors Influence On Jamesonite And Marmatite*, *Adv. Mat. Res.*, 275, 616-618.
- MA, G., 2006. *Study on flotation property of Pb-Sb-Zn-Fe sulfide by aryl thiolate collectors*. Doctoral dissertation, Central South University.
- HUANG, H., SUN, W., 2010. *Effect of 2-aminothiophenol on the separation of jamesonite and marmatite*, *Min. Sci. Technol.*, 20(3), 425-427.
- WANG, J., *Investigation on the new collector for the bulk-flotation of multy-metal sulfideore in Dachang*. Doctoral dissertation, Guangxi University.
- ÖZTÜRK, Y., BİÇAK, Ö., ÖZDEMİR, E., EKMEKÇİ, Z., 2018. *Mitigation negative effects of thiosulfate on flotation performance of a Cu-Pb-Zn sulfide ore*, *Miner. Eng.*, 122, 142-147.
- CHEN, W., CHEN, T., BU, X., CHEN, F., DING, Y., ZHANG, C., DENG, S., SONG, Y., 2019. *The selective flotation of chalcopyrite against galena using alginate as a depressant*, *Miner. Eng.*, 141, 148-105.
- ZHONG, H., HUANG, Z., ZHAO, G., WANG, S., LIU, G., CAO, Z., 2015. *The collecting performance and interaction mechanism of sodium diisobutyl dithiophosphinate in sulfide minerals flotation*, *Mater. Res. Technol.*, 4(2), 151-161.
- LAI, H., DENG, J., WEN, S., LIU, Q., 2019. *Elucidation of lead ions adsorption mechanism on marmatite surface by PCA-assisted ToF-SIMS, XPS and zeta potential*. *Miner. Eng.*, 144, 106035.
- SUI, C., RASHCHI, F., XU, Z., KIM, J., NESSET, J.E., FINCH, J.A., 1998. *Interactions in the sphalerite-Ca-SO₄-CO₃ systems*. *Colloids Surf.*, 137(1-3), 69-77.
- FINKELSTEIN, N.P., 1997. *The activation of sulphide minerals for flotation: a review*. *Int. J. Mineral Process.*, 52(2-3), 81-120.
- ZHANG, T., QIN, W., YANG, C., HUANG, S., 2014. *Floc flotation of marmatite fines in aqueous suspensions induced by butyl xanthate and ammonium dibutyl dithiophosphate*, *Trans. Nonferrous Met. Soc. China*, 24(5), 1578-1586.
- ZHAO, L., LIU, W., DUAN, H., WANG, X., FANG, P., LIU, W., ZHOU, X., SHEN, Y., 2021. *Design and selection of flotation collectors for zinc oxide minerals based on bond valence model*. *Miner. Eng.*, 160, 106681.
- CAO, Y., XIE, X., TONG, X., FENG, D., LV, J., CHEN, Y., SONG, Q., 2021. *The activation mechanism of Fe(II) ion-modified cassiterite surface to promote salicylhydroxamic acid adsorption*. *Miner. Eng.*, 160, 106707.
- DAVILA-PULIDO, G. I., URIBE-SALAS, A., G.I. 2014. *Effect of calcium, sulphate and gypsum on copper-activated and non-activated sphalerite surface properties*. *Miner. Eng.*, 55(1), 147-153.
- IGNATKINA, V.A., BOCHAROV, V.A., D'YACHKOV, F.G., 2014. *Collecting properties of diisobutyl dithiophosphinate in sulfide minerals flotation from sulfide ore*. *J. Min. Sci.*, 49(5), 795-802.
- LAGER, T., FORSSBERG, E., 2015. *Beneficiation characteristics of antimony minerals*.
- SUN, W., HAN, H., TAO, H., LIU, R., 2015. *Study on the flotation technology and adsorption mechanism of galena-jamesonite separation*, *Int. J. Min. Sci. Technol.*, 25(1), 53-57.
- ZHANG, T., QIN, W., 2015. *Floc flotation of jamesonite fines in aqueous suspensions induced by ammonium dibutyl dithiophosphate*, *J. Cent. South Univ.*, 22(4), 1232-1234.
- WEI, Q., JIAO, F., QIN, W., DONG, L., FENG, L., 2019. *Use of PASP and ZnSO₄ mixture as depressant in the flotation separation of chalcopyrite from Cu-activated marmatite*, *Physicochem. Probl. Miner. Process.*, 55(5), 1192-1194.
- ZHAO, K., WANG, X., WANG, Z., YAN, W., ZHOU, X., XU, L., WANG, C., 2019. *A novel depressant for selective flotation separation of pyrite and pyrophyllite*, *Appl. Surf. Sci.*, 487, 9-13.

- MING, P., XIE, Z., GUAN, Y., WANG, Z., LI, F., XING, Q., 2020. *The effect of polysaccharide depressant xanthan gum on the flotation of arsenopyrite from chlorite*, Miner. Eng, 157, 106551.
- XIONG, W., DENG, J., ZHAO, K., WANG, W., WANG, Y., WEI, D., 2020. *Bastnaesite, Barite, and Calcite Flotation Behaviors with Salicylhydroxamic Acid as the Collector*, Miner, 10, 282-286.
- MAN, X., OU, L., WANG, C., JIN, S., MA, X., 2019. *Flotation Separation of Diaspore and Kaolinite by Using a Mixed Collector of Sodium Oleate-Tert Dodecyl Mercaptan*, Front in Chem, 7.
- LIU, Z., 2009. *Study on electrochemistry of flotation of lead-antimony-zinc sulfide ore in dithiophosphate system*. Doctoral dissertation, 20.
- MA, X., HU, Y., ZHONG, H., WANG, S., LIU, G., ZHAO, G., 2016. *A novel surfactant S-benzoyl-N,N-diethyldithiocarbamate synthesis and its flotation performance to galena*, Appl. Surf. Sci, 365, 342-345.
- ZHAO, L., LIU, W., DUAN, H., WANG, X., FANG, P., LIU, W., ZHOU, X., SHEN, Y., 2021. *Design and selection of flotation collectors for zinc oxide minerals based on bond valence model*. Miner. Eng, 160, 106681.
- JIA, Y., HUANG, X., HUANG, K., WANG, S., CAO, Z., ZHONG, H., 2019. *Synthesis, flotation performance and adsorption mechanism of 3-(ethylamino)-N-phenyl-3-thioxopropanamide onto galena/sphalerite surfaces*, J. Ind. Eng. Chem., 77, 416-419.
- CAO, Z., YANG, Z., ZHANG, C., XIE, L., ZHAO, X., PAN, P., YUAN, Y., QI, W., HE, J., ZHANG, H., XUE, T., ZHANG, P., WEI, J., ZHANG, K., ZHAO, J., 2020. *Facile synthesis of Sb-Sb₂O₅@P@C composite and study for the supercapacitor application*, J. Mater. Sci-Mater. El, 31(3), 2406-2409.
- ZAKAZNOVA-HERZOG, V.P., HARMER, S. L., NESBITT, H.W., BANCROFT, G.M., FLEMMINGR, PRATT, A.R., 2006. *High resolution XPS study of the large-band-gap semiconductor stibnite (Sb₂S₃): Structural contributions and surface reconstruction*, Surf. Sci, 600(2), 348-351.
- FENG, B., ZHONG, C., ZHANG, L., GUO, Y., WANG, T., HUANG, Z., 2020. *Effect of surface oxidation on the depression of sphalerite by locust bean gum*, Miner. Eng, 146.
- EJTEMAEI, M., NGUYEN, A.V., 2017. *Characterisation of sphalerite and pyrite surfaces activated by copper sulphate*, Miner Eng, 100, 223-232.
- HUANG, X., JIA, Y., CAO, Z., WANG, S., ZHONG, H., 2019. *Investigation of the interfacial adsorption mechanisms of 2-hydroxyethyl dibutyldithiocarbamate surfactant on galena and sphalerite*, Colloids Surf, 583.
- PAN, G., SHI, Q., ZHANG, G., HUANG, G., 2020. *Selective depression of talc in chalcopyrite flotation by xanthan gum: Flotation response and adsorption mechanism*, Colloids Surf, 600, 29.
- LIU, D., ZHANG, G., CHEN, Y., HUANG, G., GAO, Y., 2020. *Investigations on the utilization of konjac glucomannan in the flotation separation of chalcopyrite from pyrite*, Miner. Eng, 145.
- CAO, Y., SUN, L., GAO, Z., SUN, W., CAO, X., 2020. *Activation mechanism of zinc ions in cassiterite flotation with benzohydroxamic acid as a collector*. Miner. Eng, 156,106523.